ENHANCING THE ELECTROCHEMICAL PERFORMANCE OF HIGH-VOLTAGE MATERIALS IN Li-ION CELLS USING ADDITIVE-BASED ELECTROLYTES

Cosmin UNGUREANU [1], Adina MELINTE [2], Adnana SPÎNU-ZĂULEȚ [3], Alexandru RIZOIU [4], Sébastien FANTINI [5], Christian FINK ELKJÆR [6], Mihaela BUGA[*7], Horia NECULA[8]

Lithium-ion batteries (LIB) are essential for energy storage, providing high energy density, long cycle life, and low self-discharge rates. Increasing market demand requires improvements in LIB performance, particularly in cycling stability. This study investigates carbonate-based electrolytes with additives to mitigate capacity fading due to $LiPF_6$ decomposition. The high-voltage spinel material LNMO was evaluated in half-cell configurations against metallic lithium, utilizing carbonate-based electrolytes with different additives. The Lithium Nickel Manganese Oxide (LNMO) cathode demonstrated a specific capacity of 116 mAh/g at 3C and exceeding 115 mAh g^{-1} at 1C, with over 85% capacity retention after 120 cycles, highlighting its potential to enhance LIB technology.

Keywords: Lithium-ion batteries, LNMO cathode, CR2032 half-cell, additives, electrolyte

[1] PhD Student, National Research and Development Institute for Cryogenic and Isotopic Separation, ICSI Ramnicu Valcea, ROM-EST, Romania; National University of Science and Technology POLITEHNICA Bucharest, Faculty of Energy Engineering, Bucharest, Romania, e-mail: cosmin.ungureanu@icsi.ro

[2] ACS. Eng., National Research and Development Institute for Cryogenic and Isotopic Separation, ICSI Ramnicu Valcea, ROM-EST Romania, e-mail: adina.melinte@icsi.ro

[3] PhD, National Research and Development Institute for Cryogenic and Isotopic Separation, ICSI Ramnicu Valcea, ROM-EST, Romania, e-mail: adnana.zaulet@icsi.ro

[4] PhD National Research and Development Institute for Cryogenic and Isotopic Separation, ICSI Ramnicu Valcea, ROM-EST, Romania; National University of Science and Technology POLITEHNICA Bucharest, Faculty of Chemical Engineering and Biotechnologies, e-mail: alexandru.rizoiu@icsi.ro

[5] PhD, Solvionic, Toulouse, France, email: sfantini@solvionic.com

[6] PhD, Topsoe Battery Materials, Birkerød, Region Hovedstaden, Danmark, e-mail: CHRE@topsoe.com

[7] * National Research and Development Institute for Cryogenic and Isotopic Separation, ICSI Ramnicu Valcea, ROM-EST Romania; Institute of Condensed Matter and Nanosciences Molecular Chemistry, Materials and Catalysis, Université catholique de Louvain, Belgium, e-mail: mihaela.buga@icsi.ro, mihaela-ramona.buga@uclouvain.be

[8] Prof., National University of Science and Technology POLITEHNICA Bucharest, Faculty of Energy Engineering, Bucharest, ROMANIA, e-mail: horia.necula@upb.ro

1. Introduction

Lithium-ion batteries (LIBs) have become a cornerstone of modern energy storage technologies, powering a wide array of applications ranging from portable electronics to electric vehicles (EVs) and renewable energy systems [1]. The increasing energy demands and the push for sustainable solutions require the development of high-voltage materials that can deliver superior performance and safety. Among these, $LiNi_{0.5}Mn_{1.5}O_4$ (LNMO) has emerged as a promising candidate for high-voltage cathodes due to its promising electrochemical characteristics and structural stability.

Characterized by its spinel structure, LNMO operates at a high voltage of approximately 4.7V (*vs* Li/Li^+), notably higher than conventional cathodes such as $LiMn_2O_4$ (LMO), $LiCoO_2$ (LCO), and $LiFePO_4$ (LFP). This elevated voltage can yield a theoretical capacity of around 650 Wh/kg, significantly enhancing the energy density of LIBs, making LNMO an attractive option for applications demanding higher performance. Additionally, the absence of cobalt not only reduces costs but also alleviates the ethical and environmental concerns associated with cobalt mining. While LNMO offers remarkable performance, the instability of the electrolyte during cycling presents challenges that can compromise safety and durability. The interaction between the electrolyte and the LNMO cathode can lead to the formation of unwanted by-products that contribute to capacity loss and diminished cycling stability [2, 3, 4]. Traditional carbonate-based electrolytes may not provide optimal stability under high voltage, demanding the integration of additives to enhance performance. Recent research highlights the importance of using safe and effective electrolyte formulations that include additives such as vinylene carbonate (VC) and fluoroethylene carbonate (FEC). These additives are known to stabilize the formation of a robust Cathode Electrolyte Interphase (CEI) on the surface of the LNMO cathode, mitigating the undesirable reactions that occur during charge and discharge cycles [5, 6, 7]. The addition of VC and FEC, alongside Lithium bis(oxalato)borate (LiBOB), not only improves the cycling performance but also enhances the safety of the LIB system by reducing the risk of gas evolution and thermal runaway conditions. Furthermore, incorporating LiBOB serves to enhance the overall ionic conductivity of the electrolyte while stabilizing the CEI layer, resulting in improved safety margins and extended cycle life [8, 9, 10, 11]. Studies have demonstrated that the combination of these additives leads to more stable voltage profiles and better capacity retention in half-cell configurations, emphasizing the requirement of tailored electrolyte solutions to maximize the performance of high-voltage LNMO cathodes [12].

LNMO represents a compelling high-voltage cathode material for the next generation of lithium-ion batteries. Its potential is further augmented by the careful selection of electrolytes with appropriate additives, collectively enhancing safety

and cycling performance. Ongoing research and development efforts are critical to fully harness the capabilities of LNMO and to pave the way toward more sustainable and efficient energy storage solutions.

To investigate the capabilities of lithium-ion battery technology further, this study focuses on the electrochemical performance of the high-voltage spinel material LNMO ($LiNi_{0.5}Mn_{1.5}O_4$) in CR2032 half-cell configurations. We present detailed experimental results that demonstrate how LNMO behaves under specific operating conditions, leveraging a tailored electrolyte formulation to optimize performance.

To further explore these possibilities, LNMO cathodes were tested with a carbonate-based electrolyte formulation of 1.2M $LiPF_6$ in EC (3:7) + 0.5% VC + 0.5% FEC + 0.1M LiBOB. The results indicate that the LNMO cathode attained a specific capacity exceeding 115 $mAh \cdot g^{-1}$ at 1C, with good capacity retention of over 85% after 120 cycles. This performance underscores the potential of LNMO as a promising candidate for advancing the field of lithium-ion battery technology.

2. Methodology

All materials used in this study were of analytical grade and were used without further purification. $LiNi_{0.5}Mn_{1.5}O_4$ (LNMO), was kindly provided by Haldor Topsøe. Conductive carbon (C65) was obtained from Imerys C-NERGY™, Polyvinylidene fluoride (PVdF, Solef® 5130) was sourced from Solvay, and N-Methyl-2-pyrrolidone (NMP, anhydrous, 99.5%) was purchased from Sigma-Aldrich, while the electrolyte was provided by Solvionic.

The LNMO, C65, PVdF, and NMP solvent in a 92:4:4 weight ratio slurry was homogenized using a planetary mixer under controlled temperature and vacuum. The resulting slurry was cast onto carbon-coated aluminum foil (battery grade, thickness: 15 µm, from ARMOR) using roll-to-roll coating technology (from Thank Metal, Japan). After pre-drying, the electrodes were punched into 14 mm diameter discs using a high-precision electrode cutter from El-Cell and were further dried overnight at 130°C under vacuum to ensure complete removal of any remaining moisture and residual NMP solvent. The final active mass loading was ~14.4 mg/cm^2. The cell assembly was carried out in an argon-filled glove box (Innovative Technology Inc., USA) with H_2O and O_2 content of less than 0.1 ppm. CR2032 Li-ion cells, in a half-cell configuration, used lithium metal chips (battery grade, thickness 1 mm, diameter 15.6 mm, from MSE Supplies), with a glass fiber separator (Whatman GF/D GE, Healthcare Life Sciences Whatman™) measuring 19 mm, and an excess of 1.2M $LiPF_6$ in EC (3:7) + 0.5% VC + 0.5% FEC + 0.1 M LiBOB electrolyte were assembled.

3. Results and discussion

The electrochemical characterization was conducted for three cells in parallel under the same conditions at 23°C. Capacity retention and coulombic efficiency were measured for each cell, enabling a direct comparison of their performance over the course of cycling. Galvanostatic cycling was performed within a voltage range of 3.4V to 4.8V using a Neware Battery Tester. Two testing protocols were employed: the first measured the cells performance at different rates, while the second examined cyclic stability. Following two cycles at current rates of C/5, C/2, 1C, 2C, 3C, and finally C/3, the first three cycles at a current rate of C/10 were dedicated to the formation process, Fig. 1a. Furthermore, 105 cycles at a 1C discharge rate were performed to assess cyclic stability, Fig. 1b.

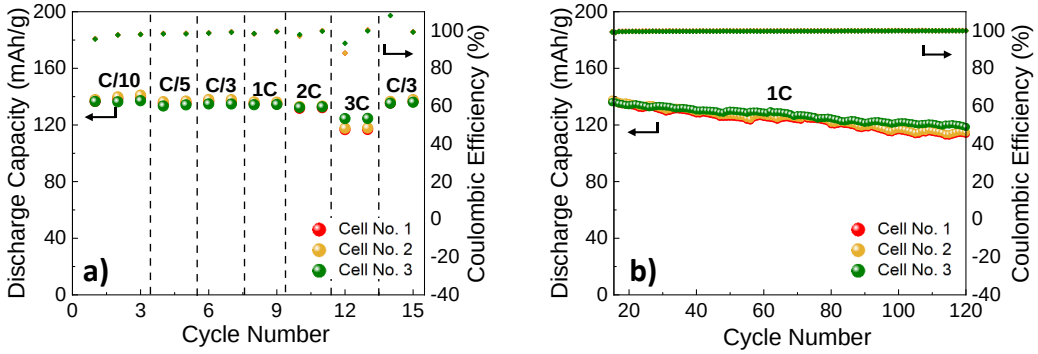

Fig. 1. a) Rate capability test at different C-rates, b) cycling stability at room temperature at 1C

The discharge capacity and coulombic efficiency following multiple cycles at different current rates are displayed in Table 1. Cell No. 1 had a discharge capacity of 136.63 mAh/g and a coulombic efficiency of 95.76%; Cell No. 2 had a capacity of 137.88 mAh/g and a coulombic efficiency of 95.26%; and Cell No. 3 had a capacity of 136.62 mAh/g and a coulombic efficiency of 95.49% following the first charge/discharge cycle at C/10. These findings suggest that the cells tested with 1.2M $LiPF_6$ in EC (3:7) + 0.5% VC + 0.5% FEC + 0.1 M LiBOB electrolyte achieved a stable cathode-electrolyte interphase layer (CEI), facilitating more effective lithium-ion transfer.

Table 1

Discharge capacity at different C-rates after rate performance protocol

	Cell No.1		Cell No.2		Cell No.3	
	Discharge Capacity (mAh/g)	Coulombic Efficiency (%)	Discharge Capacity (mAh/g)	Coulombic Efficiency (%)	Discharge Capacity (mAh/g)	Coulombic Efficiency (%)
2nd cycle @ C/10	138.54	97.72	139.81	97.72	136.31	97.67

5th cycle @ C/5	135.63	98.54	136.88	98.22	134.17	98.24
7th cycle @ C/3	136.63	99.33	137.88	99.31	134.80	99.11
9th cycle @ 1C	134.86	99.63	136.10	99.20	134.44	99.40
11th cycle @ 2C	132.18	99.93	133.39	99.01	132.84	99.63
13th cycle @ 3C	116.81	100.31	117.88	99.11	124.62	99.82
15th cycle @ C/3	136.63	99.40	137.88	99.40	136.04	99.18

The charge/discharge curves of the three half-cells at different cycle counts are presented in Fig. 2a. Fig. 2b shows the capacity retention. After 120 cycles, the first two cells exhibited a capacity retention of 84%, while the third cell, demonstrated a capacity retention of 86%.

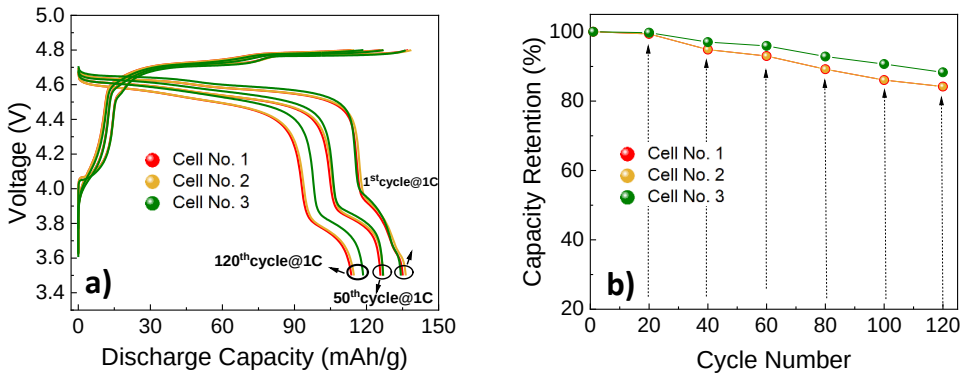

Fig. 2. a) Charge/discharge profiles at 1 C-rate after the 1st, 50th, and 120th cycles. b) Capacity retention after 120 cycles for all cells

The capacities measured at 1C after the eighth cycle are shown in Table 2. The first cell recorded a capacity of 135.09 mAh/g, the second cell recorded 136.33 mAh/g, and the third cell, 134.80 mAh/g. Following the 50th cycle at the same current rate, the discharge capacities were as follows: 125.81 mAh/g for the first cell, 126.97 mAh/g for the second cell, and 126.88 mAh/g for the third cell. After completing 120 cycles of charging and discharging, the capacities of the three cells were measured at 113.72 mAh/g, 114.77 mAh/g, and 119.28 mAh/g, respectively. Notably, all tested cells demonstrated a coulombic efficiency greater than 98%.

Table 2

Discharge capacity at different c-rate

	Cell No.1		Cell No.2		Cell No.3	
	Discharge Capacity (mAh/g)	Coulombic Efficiency (%)	Discharge Capacity (mAh/g)	Coulombic Efficiency (%)	Discharge Capacity (mAh/g)	Coulombic Efficiency (%)
8th cycle @ 1C	135.09	98.34	136.33	99.20	134.80	99.11
50th cycle @ 1C	125.81	99.85	126.97	99.97	126.88	99.79
120^{ed} cycle @ 1C	113.72	100.00	114.77	99.52	119.28	99.85

The derived dQ/dV profile for the first charge/discharge cycle of the three tested cells is presented in Fig. 3, illustrating the oxidation and reduction reactions occurring within the cells. This profile reveals three distinct peaks in the specified voltage range. The two peaks observed at potentials of approximately 4.68V to 4.76V during charging and 4.65V to 4.70V during discharging correspond to the redox processes involving nickel, specifically the Ni^{2+}/Ni^{3+} and Ni^{3+}/Ni^{4+} transitions. The peak observed at approximately 4.0V is attributed to the redox transition of Mn^{3+}/Mn^{4+} [13].

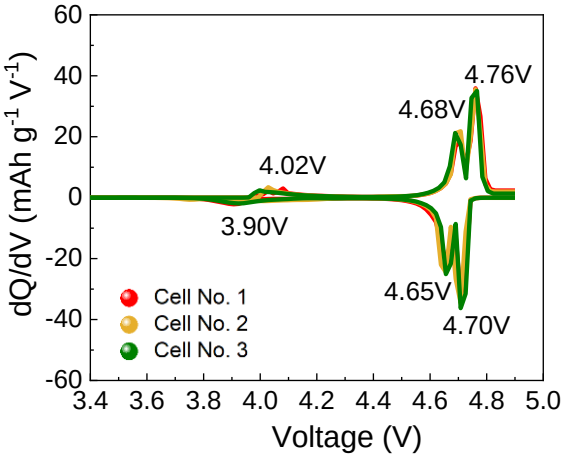

Fig. 3. Differential capacity analysis (dQ/dV) for the first cycle at C/10

Electrochemical Impedance Spectroscopy (EIS) measurements were conducted using a Solartron 1470E Multi-Channel Potentiosat over a frequency range from 500 kHz to 100 mHz, with a current amplitude of 10 mV. The impedance curves exhibit three distinct components: a semicircular region at high to medium frequencies (between 1000 Hz and 0.1 Hz), which corresponds to Li-ion

migration through the solid-electrolyte interphase (SEI) film resistance; a straight sloping line at low frequencies (< 0.1 Hz), related to the charge transfer resistance of Li ions in the bulk of the active material and the Warburg impedance (W); an Ohmic region at frequencies greater than 1000 Hz, associated with the internal resistance of each cell [14]. Notably, the Ohmic resistance showed an increase in value between the pre- and post-galvanostatic cycling, which can be attributed to changes in the electrode structure.

The contact resistance and charge transfer resistance values obtained both before and after the galvanostatic cycling are summarized in Table 3. Both resistance values increased during the galvanostatic cycling, indicating the aging process of the electrode and the electrolyte.

Table 3

Electrochemical Impedance Resistance

	Cell No.1		Cell No.2		Cell No.3	
	Contact Resitance (Ω)	Charge Transfer Resistance (Ω)	Contact Resitance (Ω)	Charge Transfer Resistance (Ω)	Contact Resitance (Ω)	Charge Transfer Resistance (Ω)
Before electrochemical testing	6.95	51.04	6.85	56.70	4.91	48.02
After 120th cycles	14.09	186.06	9.56	197.99	10.23	140.53

The results of the impedance experiment are shown visually as Nyquist plots in Fig. 3a-b, both before and after galvanostatic cycling for each of the three tested cells. For the fresh cells, the contact resistances were measured at 6.95 Ω, 6.85 Ω, and 4.91 Ω, respectively.

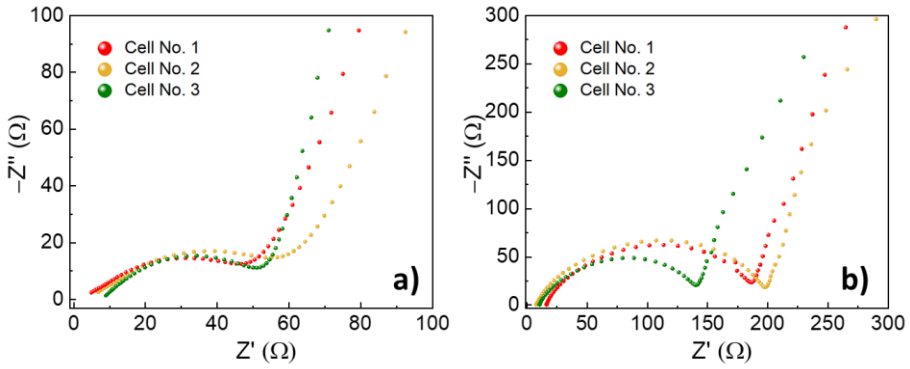

Fig. 4. EIS showing the Nyquist plots of the LNMO/Li configuration: a) before electrochemical testing; b) after galvanostatic cycling, at 23°C

These values increased to 14.09 Ω, 9.56 Ω, and 10.23 Ω during galvanostatic cycling. After completing 120 charge/discharge cycles, a significant increase in contact resistance was observed.

The following formula can be used to determine the diffusion coefficient (D_{Li}^{+}) for lithium ions from the Warburg area, which is the low-frequency region in the EIS spectra [15].

$$D_{Li}^{+} = \frac{R^2 \cdot T^2}{2 \cdot A^2 \cdot n^4 \cdot F^4 \cdot C^2 \cdot \sigma^2} \tag{1}$$

where A is the electrode surface area (1.539 cm^2), n is the number of electrons transferred per molecule of active material, F is the Faraday constant (96500 C/mol), C is the molar concentration of Li-ion in active material, R is the gas constant (8.31415 J/mol K), and σ is the Warburg factor, which can be obtained from the slope of the linear of Z' vs. $\omega^{-1/2}$, Fig. 5.

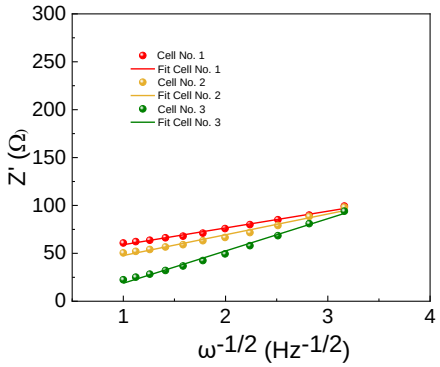

Fig. 5. Linear fitting of the Z' vs. $\omega^{-1/2}$

The diffusion coefficients for the tested samples are 2.49×10^{-11} for cell no. 1, 2.38×10^{-11} for cell no. 2, and 1.55×10^{-11} for cell no. 3. These findings align with the galvanostatic cycling results, indicating that ionic diffusion is fastest in cell no. 3.

4. Conclusions

In conclusion, the LNMO/Li cells have demonstrated excellent electrochemical performance after 120 cycles, achieving a capacity retention rate of 84%. The ability to attain discharge capacities of 132 mAh/g at 2C and 116 mAh/g at 3C highlights the remarkable electrochemical properties of the LNMO

material under varying conditions. The incorporation of electrolyte additives significantly enhanced the performance of the cells across multiple aspects. These additives improve ionic conductivity, facilitating better ion transport and leading to higher discharge capacities during cycling. Additionally, they contribute to cycling stability by stabilizing the electrolyte and minimizing decomposition processes, which prolong the lifespan of the cell. By reducing voltage polarization, these additives also enhance the efficiency of energy usage, while specific types can inhibit detrimental side reactions that may degrade cell performance over time. Furthermore, the enhanced rate capability provided by these additives allows LNMO cathodes to effectively deliver higher capacities, making them suitable for high-power applications. Overall, the strategic implementation of electrolyte additives is crucial for optimizing the electrochemical characteristics of LNMO, driving advancements in lithium-ion technology.

Acknowledgments

This work was supported by the HYDRA project, which received funding from the European Union's Horizon 2020 research and innovation program under Grant Agreement No. 875527. Additional support came from the Romanian Ministry of Research, Innovation, and Digitalization through project PN 23 15 02 01 (BatNaS) and from a grant provided by the European Regional Development Fund as part of the Competitiveness Operational Program for the project "From Nano to Macro in Hydrogen Energy-Extension of the National Center for Hydrogen and Fuel Cells-HyRo 2.0," SMIS 127318, project no. 308/2020.

R E F E R E N C E S

[1] *J. Amici, et al.,* A Roadmap for Transforming Research to Invent the Batteries of the Future Designed within the European Large Scale Research Initiative BATTERY 2030+, Adv. Energy Mater, Vol. **12**, 2102785, 2022.

[2] *Z. Tong, X. Zhu*, A patent landscape analysis on the high-voltage spinel $LiNi_{0.5}Mn_{1.5}O_4$ for next-generation lithium-ion batteries, Next Energy, Vol. **5**, 100158, 2024.

[3] *M. D. Bouguern, A. Kumar, K. Zaghib*, The critical role of interfaces in advanced Li-ion battery technology: A comprehensive review, Journal of Power Sources, Vol. **623**, 23545, 2024.

[4] *C. Lin, S. Lin,* A first-principles study on stabilizing disordered $LiNi_{0.5}Mn_{1.5}O_4$ cathode material by doping, Journal of Energy Storage, Vol. **83**, 110637, 2024.

[5] *M. Hekmatfar, I. Hasa, R. Eghbal, D.V. Carvalho, A. Moretti, S. Passerini*, Effect of Electrolyte Additives on the $LiNi_{0.5}Mn_{0.3}Co_{0.2}O_2$ Surface Film Formation with Lithium and Graphite Negative Electrodes, Adv. Mater. Interfaces, Vol. **7**, 1901500, 2020.

[6] L. Hu, Z. Zhang, K. Amine, Fluorinated electrolytes for Li-ion battery: An FEC-based electrolyte for high voltage $LiNi_{0.5}Mn_{1.5}O_4$/graphite couple, Electrochemistry Communications, Vol. **35**, 76-79, 2013.

[7] *D. Pritzl et al.,* Analysis of Vinylene Carbonate (VC) as Additive in Graphite/$LiNi_{0.5}Mn_{1.5}O_4$ Cells, J. Electrochem. Soc., Vol. **164**, A2625, 2017.

[8] *X. Cui, F. Tang, C. Li, Y. Zhang, P.Wang, H. Feng, J. Zhao, F. Li, S. Li,* Improving Mn tolerance of lithium-ion batteries by using lithium bis(oxalato)borate-based electrolyte, Electrochimica Acta, Vol. **253,** 291-301, 2017.

[9] A. *Hofmann, A. Höweling, N. Bohn, M. Müller, J.R.Binder, T. Hanemann*, Additives for Cycle Life Improvement of High-Voltage LNMO-Based Li-Ion Cells, ChemElectroChem, Vol. **6**, 5255–5263, 2019.

[10] *N.P. W. Pieczonka, L. Yang, M.P. Balogh, B.R. Powell, K. Chemelewski, A. Manthiram, S.A. Krachkovskiy, G.R. Goward, M. Liu, J.-H. Kim*, Impact of Lithium Bis(oxalate)borate Electrolyte Additive on the Performance of High-Voltage Spinel/Graphite Li-Ion Batteries, J. Phys. Chem. C, Vol. **117**, 22603−22612, 2013.

[11] *Z. Xiao, J. Liu, G. Fan, M. Yu, J. Liu, X. Gou, M. Yuan, F. Cheng,* Lithium bis(oxalate)borate additive in the electrolyte to improve Li-rich layered oxide cathode materials, Mater. Chem. Front., Vol. **4**, 1689-1696, 2020.

[12] *X. Deng, J. Li, P. Lai, S. Kuang, J. Liu, P. Dai, H. Hua, P. Dong, Y. Zhang, Y. Yang, J. Zhao,* Tailored interface composition improves the integrity of electrode/electrolyte interphases for high-voltage Ni-rich lithium metal batteries in a sulfolane-based electrolyte, Chemical Engineering Journal, Vol. **465**, 142907, 2023.

[13] *M. T. Nguyen, H. Q. Pham, J. A. Berrocal, I. Gunkel, U. Steiner,* An electrolyte additive for the improved high voltage performance of $LiNi_{0.5}Mn_{1.5}O_4$ (LNMO) cathodes in Li-ion batteries, Journal of Materials Chemistry, Vol. **11**, 7670, 2023.

[14] *P. Iurilli, C. Brivio, V. Wood,* On the use of electrochemical impedance spectroscopy to characterize and model the aging phenomena of lithium-ion batteries: a critical review, Journal of Power Sources, Vol. **505**, 229860, 2021.

[15] *C. Zhang, C. Liu, X. Nan, H. Song, Y. Liu, C. Zhang, G. Cao,* Hollow−Cuboid Li3VO4/C as High-Performance Anodes for Lithium - Ion Batteries, Applied Materials & Interfaces, Vol. **8**, 680-688, 2016.